CORE
Metadata, citation and similar papers at core.ac.uk
Provided by NASA Technical Reports Server

NASA TECHNICAL NOTE

NASA TN D-2278

C. 1

LOAN COPY: RETURN
AFWL (WLIL-2)
KIRTLAND AFB, N ME

01549S7

TECH LIBRARY KAFB, NM

NASA TN D-2278

ANALYTICAL INVESTIGATIONS OF COIL-SYSTEM DESIGN PARAMETERS FOR A CONSTANT-VELOCITY TRAVELING MAGNETIC WAVE PLASMA ENGINE

by Raymond W. Palmer, Robert E. Jones, and George R. Seikel

Lewis Research Center
Cleveland, Ohio

NATIONAL AERONAUTICS AND SPACE ADMINISTRATION • WASHINGTON, D. C. • MAY 1964

TECH LIBRARY KAFB, NM
0154957

ANALYTICAL INVESTIGATIONS OF COIL-SYSTEM DESIGN PARAMETERS FOR A CONSTANT-VELOCITY TRAVELING MAGNETIC WAVE PLASMA ENGINE

By Raymond W. Palmer, Robert E. Jones,
and George R. Seikel

Lewis Research Center
Cleveland, Ohio

NATIONAL AERONAUTICS AND SPACE ADMINISTRATION

For sale by the Office of Technical Services, Department of Commerce,
Washington, D.C. 20230 -- Price $1.00

ANALYTICAL INVESTIGATIONS OF COIL-SYSTEM DESIGN PARAMETERS FOR A CONSTANT-VELOCITY TRAVELING MAGNETIC WAVE PLASMA ENGINE

by Raymond W. Palmer, Robert E. Jones, and George R. Seikel

Lewis Research Center

SUMMARY

Results of an analytical study of the design parameters are presented for one of the simplest methods of producing a traveling magnetic wave. This method is to excite a linear array of coils with polyphase radiofrequency electric current.

The exact and approximate equations that describe the axial and the radial components of the magnetic field are developed with the presence of a plasma neglected. The approximate equations are shown to be valid for a value of the accelerator to coil radius ratio as large as 0.5. A Fourier decomposition of the total magnetic wave shows that this wave is composed of an infinite series of waves of diminishing amplitude running opposite to each other at different velocities. The presence of magnetic waves other than the design magnetic wave, as well as the variation of the average magnetic intensity level, forms the basis for the definition of a quality factor with which all similar coaxial coil systems may be compared. For a given amount of coil power consumption, the greatest amount of magnetic energy available for useful plasma acceleration occurs at a coil-radius to magnetic-wave-wavelength ratio of 0.3 for a value of accelerator-coil radius ratio of zero (centerline). This optimum value is increased to 0.35 when the accelerator-coil radius ratio is increased to 0.5. At this optimum value, the useful energy in the magnetic wave is independent of the number of phases per wavelength when that number is greater than three. The quality factor also applies as an approximate scaling law and indicates that properly designed larger coil systems will produce the magnetic energy more efficiently than smaller systems.

INTRODUCTION

Mission analyses indicate a need for reliable electric propulsion systems with thrustor specific impulses above 1000 seconds. The traveling magnetic wave plasma engine is one of several types being studied for producing thrusts in this specific-impulse range.

The principle of operation of the traveling magnetic wave plasma engine is basically simple. Currents are induced in a plasma when a moving magnetic wave passes through it. These induced currents then interact with the moving magnetic field to produce a body force that tends to drag the plasma with the field. Plasma engines of this type are analogous to alternating-current linear-induction motors. These plasma motors differ essentially only in the production of the traveling magnetic wave, or stator, to which the plasma, or rotor, is coupled.

The methods of producing traveling magnetic waves encompass a variety of techniques. Reference 1, for example, describes a system that produces a magnetic wave of nearly constant amplitude and velocity, which uses two radio-frequency transmitters maintained 90° apart in electrical current phase. Reference 2 describes a system that employs a solenoidal transmission line terminated in its characteristic impedance. Reference 3 describes an axisymmetric system of coils with increasing coil spacing capable of producing an accelerating magnetic wave. The relative merit of any particular wave-producing system, however, is as yet unproved.

It is the purpose of this report to discuss one simple method of producing a continuous traveling magnetic wave and to analyze the effect of several coil system parameters on the smoothness and strength of the wave. The presence of the plasma may be neglected as a first approximation, since the induced field in the plasma must be small compared with the applied field. Otherwise, the applied field penetrates and accelerates the plasma only in a thin annular skin. Preliminary results of this study were employed in the construction of the plasma engine discussed in reference 1.

The coil system that is considered consists of a number of identical single-turn loops n_T mounted coaxially with a constant separation distance between adjacent loops δ; each coil carries sinusoidal alternating current of constant amplitude and frequency but differs in electrical current phase from an adjacent coil by a constant amount $\Delta\varphi$. The quantity $\Delta\varphi$ is $2\pi/N$, where N is the number of phases or coils per wavelength of the system.

The magnetic field of the coil system is obtained by superimposing the fields of the n_T single-turn loops. The resulting axial magnetic profiles for coil systems of finite and infinite extent are examined at an instant of time to obtain "snapshots" of the traveling magnetic wave. In addition, the magnitude and phase angle of the magnetic field maximum are investigated. For systems of infinite extent, the axial magnetic profile is decomposed into a series of constant-amplitude constant-velocity magnetic waves traveling in both directions. Since the plasma acceleration process is primarily dependent on the radial magnetic field, the corresponding series is obtained for this field by utilizing Maxwell's divergence equation. Quality factors are defined to compare all similar coaxial coil systems on the basis of maximizing the energy in the radial component of the design magnetic wave and minimizing undesirable waves. These factors determine the values of coil system parameters that maximize the amount of energy available for useful plasma acceleration for a given amount of electrical power consumed in the coil system.

DEVELOPMENT OF EQUATIONS

Approximate Magnetic Field of Single-Turn Loop

Figure 1 depicts a single-turn loop of radius a carrying a current I. The axial and radial magnetic flux densities at any field point P located an axial distance d and a radial distance r from the geometric center of the loop are given in reference 4 as

$$B_z = \frac{\mu I}{2\pi\left[(r + a)^2 + d^2\right]^{1/2}}\left[K(k) + \frac{a^2 - r^2 - d^2}{(a - r)^2 + d^2}E(k)\right] \tag{1}$$

and

$$B_r = \frac{\mu I d}{2\pi r\left[(r + a)^2 + d^2\right]^{1/2}}\left[\frac{a^2 + r^2 + d^2}{(a - r)^2 + d^2}E(k) - K(k)\right] \tag{2}$$

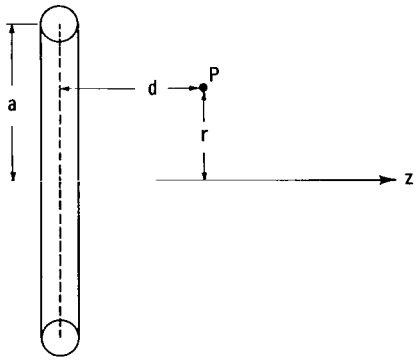

Figure 1. - One-turn-loop geometry.

respectively. (All symbols are defined in appendix A.)

In equations (1) and (2), K(k) is the complete elliptic integral of the first kind and E(k) is the complete elliptic integral of the second kind. The modulus k is defined by

$$k^2 = \frac{4ar}{(r + a)^2 + d^2}$$

where $k^2 < 1$.

Equations (1) and (2) may be nondimensionalized by employing the dimensionless variables $\rho = r/a$ and $\bar{d} = d/a$ and dividing each equation by B_0, which is the flux density produced at the geometric center of an identical single-turn loop carrying a steady current I_0. Equations (1) and (2) may be written as

$$\frac{B_z}{B_0} = \frac{\frac{I}{I_0}}{\pi\left[\rho(\rho + 2) + \bar{b}\right]^{1/2}}\left[K(k) + \frac{(2 - \rho^2) - \bar{b}}{\rho(\rho - 2) + \bar{b}}E(k)\right] \tag{3}$$

and

$$\frac{B_r}{B_0} = \frac{[\bar{b} - 1]^{1/2}\frac{I}{I_0}}{\pi\rho\left[\rho(\rho + 2) + \bar{b}\right]^{1/2}}\left[\frac{\rho^2 + \bar{b}}{\rho(\rho - 2) + \bar{b}}E(k) - K(k)\right] \tag{4}$$

where

$$\bar{b} = 1 + \bar{d}^2 \tag{5}$$

The modulus k in nondimensional form is defined by

$$k^2 = \frac{4\rho}{\rho(\rho + 2) + \bar{b}} \tag{6}$$

where $k^2 < 1$.

Later calculations for multiphase coil systems would prove extremely difficult if equations (3) and (4) were retained in their exact form. Therefore, a convenient approximation was made in the form of a power series expansion in ρ. It is shown in appendix B that, if terms of order greater than ρ^2 are neglected,

$$\frac{B_z}{B_0} = \frac{I\bar{b}^{-3/2}}{I_0}\left[1 - \rho^2\left(3\bar{b}^{-1} - \frac{15}{4}\bar{b}^{-2}\right)\right] \tag{7}$$

$$\frac{B_r}{B_0} = \frac{3\rho}{2}\frac{I}{I_0}\left(\frac{\bar{b}-1}{\bar{b}^5}\right)^{1/2}\left[1 - \frac{5}{2}\rho^2\bar{b}^{-1}\left(1 - \frac{7}{4}\bar{b}^{-1}\right)\right] \tag{8}$$

Figures 2 and 3 compare calculations of the approximate and the exact

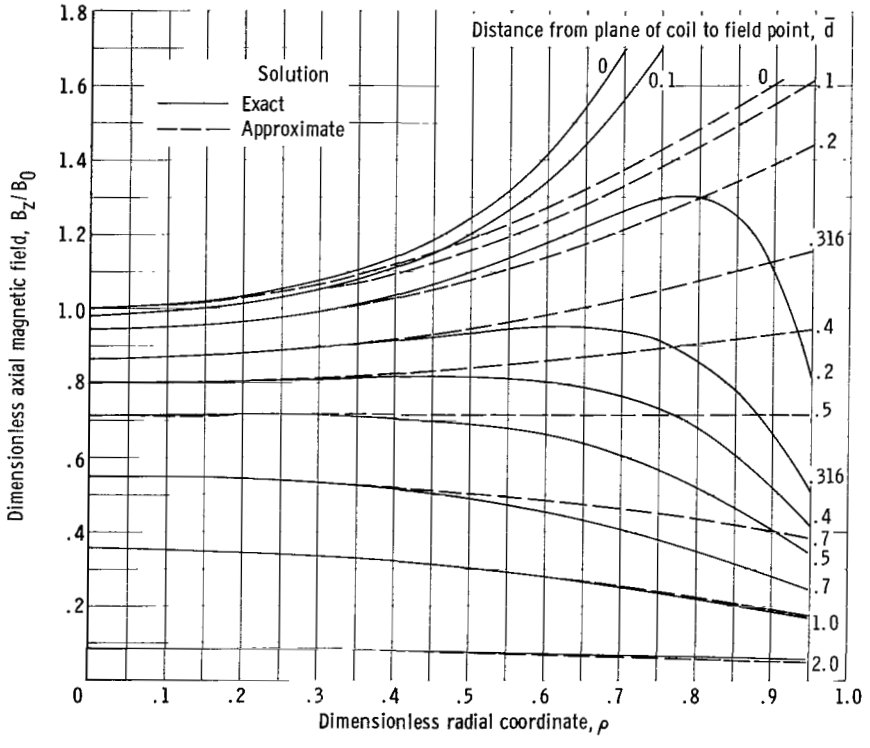

Figure 2. - Comparison of exact and approximate solutions of dimensionless axial magnetic field.

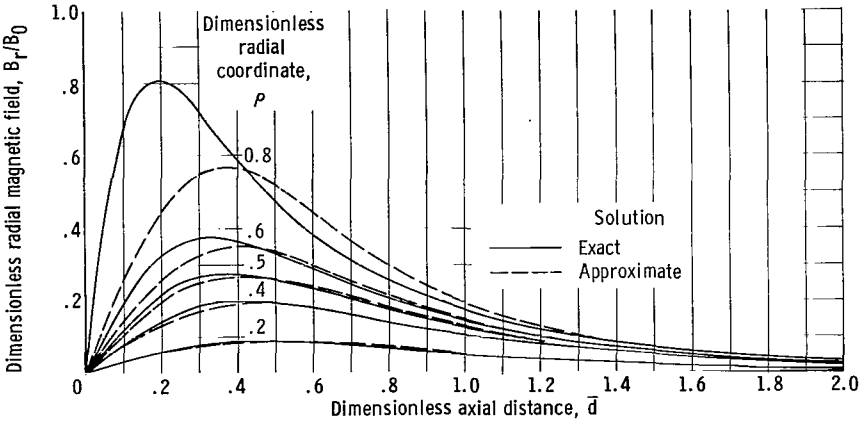

Figure 3. - Comparison of exact and approximate solutions of dimensionless radial magnetic field.

dimensionless field equations for a single-turn loop. For the axial magnetic field (fig. 2), the approximate solution agrees within 10 percent with the exact solution for values of the radius ratio to 0.6. For the radial component of the magnetic field (fig. 3), these two solutions agree within 10 percent for values of the radius ratio as large as 0.5. Generally, the approximate solution agrees quite well with the exact solution at larger values of the radius ratio when the distance between the plane of the coil and the field point is increased ($d \to \infty$).

These two figures indicate that the approximate solution is generally useful at values of the dimensionless radial coordinate to 0.5 for any axial distance.

Axial Magnetic Field of Coil System

The coil system that is used to generate a traveling magnetic wave is shown in figure 4. This system consists of $n_T = n_+ + n_-$ identical single-turn loops in a coaxial array such that a constant spacing δ is maintained between adjacent coils. Each coil carries maximum sinusoidal current I_0 at an angular frequency ω. In addition, each coil differs in electrical current phase from an adjacent coil by a constant amount $\Delta\varphi$. The reference, or zero phase, coil is located at $z = 0$, and the current phase increases positively to the right, negatively to the left. Thus, the current in the n^{th} coil is written as

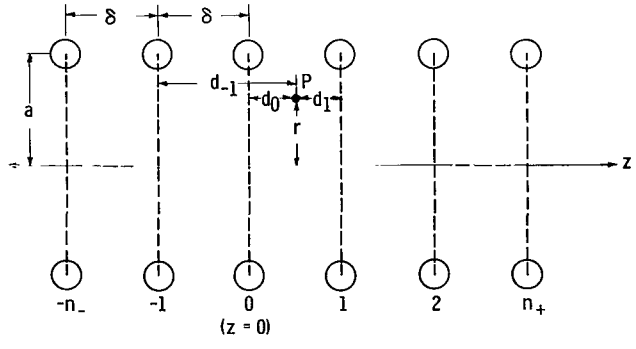

Figure 4. - Multiple-coil-system geometry.

$$I_n = I_0 \cos(\omega t - n\,\Delta\varphi) \qquad (9)$$

The axial magnetic flux density produced by this arrangement of coils at a field point P, located an axial

distance z and a radial distance r from the center of the reference phase, is obtained by summing the axial magnetic flux density of each coil at the field point. Substitution of equation (9) into equation (7) and summation over the total number of coils yield the nondimensional expression

$$\frac{B_z}{B_0} = \sum_{-n_-}^{n_+} b_n^{-3/2}\left[1 - \rho^2\left(3b_n^{-1} - \frac{15}{4}\,b_n^{-2}\right)\right]\cos(\omega t - n\,\Delta\varphi) \tag{10}$$

where

$$b_n = 1 + \bar{d}_n^2 \tag{11}$$

The term $\bar{d}_n$ in equation (11) is the dimensionless axial distance from the n^{th} coil to the field point and can be written as

$$\bar{d}_n = \left|\frac{z - n\delta}{a}\right| \tag{12}$$

Equations (10) to (12) may be more conveniently written by defining a dimensionless axial coordinate

$$\zeta = \frac{z}{\lambda} \tag{13}$$

and by noting that

$$N = \frac{2\pi}{\Delta\varphi} = \frac{\lambda}{\delta} \tag{14}$$

where λ, the magnetic-wave wavelength, is the distance between two coils of identical phase angle and N is the number of coils or phases per wavelength. With the use of equations (13) and (14), equations (10) and (12) may be rearranged and written as

$$\frac{B_z}{B_0} = \sum_{-n_-}^{n_+} F_n \cos\left(\omega t - 2\pi\,\frac{n}{N}\right) \tag{15}$$

where

$$F_n = b_n^{-3/2}\left[1 - \rho^2\left(3b^{-1} - \frac{15}{4}\,b_n^{-2}\right)\right]$$

and

$$b_n = 1 + \left(\frac{\lambda}{a}\right)^2\left(\zeta - \frac{n}{N}\right)^2$$

Equation (15) may also be written as

$$\frac{B_z}{B_0} = \frac{\overline{B}}{B_0} \cos(\omega t - \Phi) \tag{16}$$

where $\overline{B}/B_0$ is the nondimensional maximum amplitude of the traveling magnetic wave and Φ is the phase angle of the maximum magnetic intensity. These terms are given by

$$\frac{\overline{B}}{B_0} = \left(C_1^2 + C_2^2\right)^{1/2} \tag{17}$$

and

$$\Phi = \tan^{-1} \frac{C_1}{C_2} \tag{18}$$

where

$$C_{\left\{\begin{smallmatrix}1\\2\end{smallmatrix}\right\}} = \sum_{-n_-}^{n_+} F_n \left\{\begin{smallmatrix}\sin\\\cos\end{smallmatrix}\right\} \frac{2\pi n}{N} \tag{19}$$

Coil Systems of Infinite Extent and Number of Phases Per Wavelength Approaching Infinity

No limit need be placed on the number of coils in the coil system. Figure 4 could be considered a doubly infinite array of coils about the point $z = 0$. In this situation $n_+ = n_- = \infty$.

It is of interest to consider a limiting case in which the magnetic wave is produced by an infinite number of coils per wavelength. The concept of an infinite number of coils per wavelength implies that the phase angle between adjacent current loops approaches zero, the distance between adjacent coils approaches zero, and the number of coils per wavelength approaches infinity.

If $\overline{\xi}_n = (n/N) - \zeta$ is substituted into equation (19) and the definitions of equation (15) are used, the result is

$$C_{\left\{\begin{smallmatrix}1\\2\end{smallmatrix}\right\}} = \sum_{-\infty}^{\infty} F_n \left\{\begin{smallmatrix}\sin\\\cos\end{smallmatrix}\right\} 2\pi(\overline{\xi}_n + \zeta) \tag{20}$$

where

$$b_n = 1 + \left(\frac{\lambda}{a}\,\bar{\xi}_n\right)^2$$

Employing the general definition of a definite integral and noting that

$$\Delta\bar{\xi}_n = \bar{\xi}_n - \bar{\xi}_{n-1} = \frac{1}{N}$$

yield the relation

$$\lim_{N\to\infty} C\begin{Bmatrix}1\\2\end{Bmatrix} = N\int_{-\infty}^{\infty} F\begin{Bmatrix}\sin\\\cos\end{Bmatrix}2\pi(\bar{\xi} + \zeta)\,d\bar{\xi} \tag{21}$$

where F and b are now continuous functions of the axis ζ and the dummy variable $\bar{\xi}$. Expanding the trigonometric functions and noting that b and F are even functions of $\bar{\xi}$ give, from equation (21), the relation

$$\lim_{N\to\infty} C\begin{Bmatrix}1\\2\end{Bmatrix} = 2N\begin{Bmatrix}\sin\\\cos\end{Bmatrix}2\pi\zeta\int_0^{\infty} F\cos 2\pi\bar{\xi}\,d\bar{\xi} \tag{22}$$

where

$$F = F(b,\rho)$$

and

$$b = 1 + \left(\frac{\lambda}{a}\,\bar{\xi}\right)^2$$

Substitution of equation (22) into equations (17) and (18) yields

$$\lim_{N\to\infty}\frac{\bar{B}}{B_0} = 2N\int_0^{\infty} F\cos 2\pi\bar{\xi}\,d\bar{\xi} \tag{23}$$

and

$$\lim_{N\to\infty}\Phi = 2\pi\zeta \tag{24}$$

DISCUSSION OF TOTAL MAGNETIC-WAVE PROFILES

Magnetic-Wave Instantaneous Profiles

The axial magnetic wave produced on the centerline of a typical six-coil six-phase system is shown in figure 5 for several phases of the cycle. These curves, obtained from equation (15), demonstrate the motion of the magnetic wave through this coil system. It is shown in the section QUALITY FACTOR DEFINITIONS that the nearly sinusoidal shape and nearly constant velocity of the particular wave shown in figure 5 is the result of choosing a value close to the optimum value of the coil-radius to magnetic-wave-wavelength ratio. The selection of a value of the coil-radius to magnetic-wave-wavelength ratio far from the optimum value would have yielded a much more distorted wave.

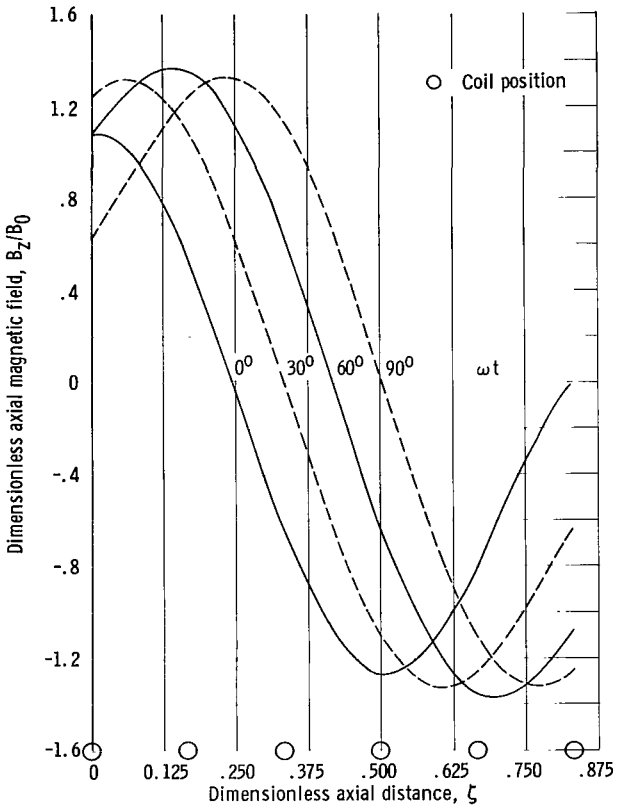

Figure 5. - Instantaneous curves of dimensionless axial magnetic field for six-coil six-phase system. Coil-wavelength ratio, 0.245.

Variation of Magnetic Field Amplitude and Phase Angle

From equation (16) it is seen that in order for a coil system to generate a perfect magnetic wave, which is defined as a wave with a constant amplitude and a constant velocity, both the dimensionless amplitude and the slope of the phase angle must be independent of distance. Examination of equations (23) and (24) reveals that infinitely long systems with the number of phases per wavelength approaching infinity possess these two requirements. In no other cases investigated, however, were these requirements entirely met.

Equations (17) and (18), which describe the magnetic-intensity profiles and phase-angle variations for coil systems of both finite and infinite extent, were programed for a high-speed digital computer with a wide variation in the number of coils per wavelength, the total number of coils, and the coil-radius to magnetic-wave-wavelength ratio. For simplicity, these computations were made only for the centerline magnetic field ($\rho = 0$). At $\rho = 0$, the calculations are not only simplified but also exact.

The cases computed are shown in table I. The number of coils listed for the systems of infinite extent is the number of coils required to approximate

TABLE I. - VARIABLES FOR FINITE AND

INFINITE COIL SYSTEMS

Number of phases or coils per wavelength, N	Ratio of coil-radius to magnetic-wave-wavelength, a/λ	Coil system,	
		Finite	Infinite
		Total number of coils, n_T	
12	0.555	12	300
	.333	--	240
	.238	12	240
	.111	--	100
	.083	12	70
	.055	--	70
	.042	--	60
	.028	--	40
6	0.666	6	300
	.333	--	150
	.248	6	150
	.222	--	150
	.167	--	100
	.111	6	70
	.083	--	60
	.055	--	40
4	0.500	4,8,12	200
	.333	↓	150
	.250		150
	.166		100
	.125		100
	.083		60

closely an infinite coil array; that is, consideration of more coils than the number listed did not affect the results for the dimensionless axial magnetic flux density amplitude and the phase angle of the maximum of the magnetic intensity to within five significant figures.

Coil systems of infinite extent. - The variation of the dimensionless amplitude with the dimensionless axial coordinate from equations (17) and (19) is shown in figure 6 for several values of the coil-radius to magnetic-wave-wavelength ratio for four, six, and twelve coils per wavelength. The associated variation in magnetic phase angle from equations (18) and (19) is shown in figure 7. Several important qualitative characteristics are apparent from these figures.

Figure 6 indicates that the average level of the magnetic intensity maximizes at some value of the coil radius to wavelength ratio. At large values of this ratio, the combination of close coil spacing and different current phase between adjacent coils gives rise to destructive interference. At small values, each coil tends toward independent operation. This effect may be seen in figure 6 by noting the low value of the dimensionless axial flux density amplitude between coils and that the phase (shown in fig. 7) approaches a constant value

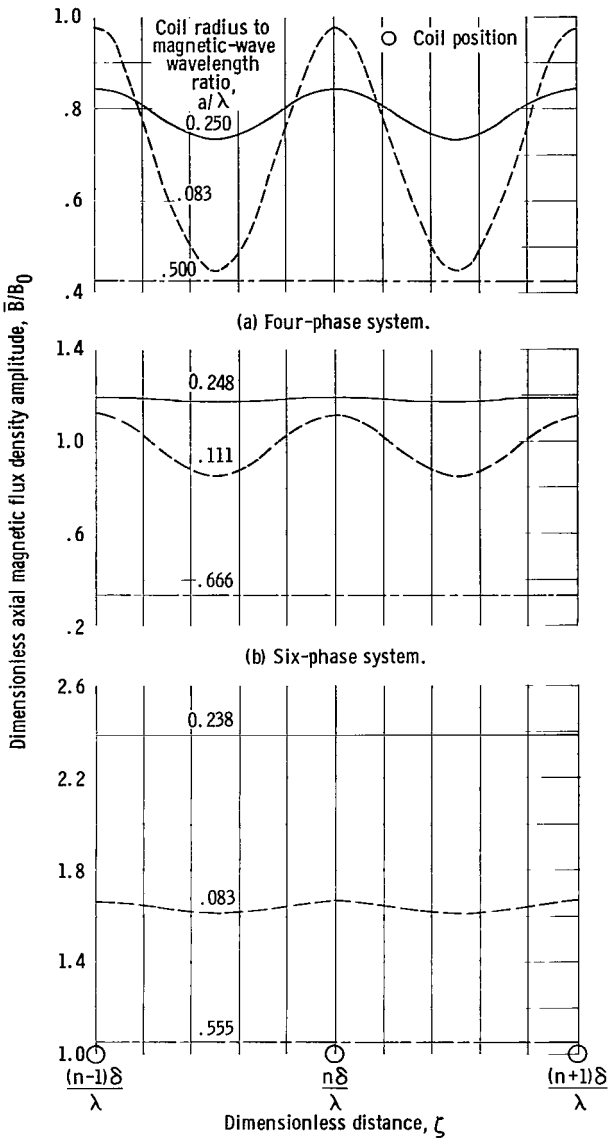

Figure 6. - Magnetic intensity envelopes for coil systems of infinite extent.

under each coil as the coil-radius to magnetic-wave wavelength ratio is decreased.

Finally, it can be seen that the deviation, or ripple, about the average magnetic intensity level is increased with decreasing coil-radius to magnetic-wave-wavelength ratio and number of coils per wavelength. This characteristic is explained on the basis of superposition as was done previously. The physical significance of this deviation, or ripple, however, is that the total wave may be analyzed in terms of a series of constant-amplitude constant-velocity sinusoidal magnetic waves running in either direction within the wave-producing system.

These general characteristics, namely, the maximization of the average magnetic amplitude and the existence of several waves within the system, were the basis for the definition of several figures of merit useful in the comparison of magnetic waves produced by similar coil systems.

Coil systems of finite extent. - Figure 8 shows the variation of wave amplitude with dimensionless distance for a number of coil systems of finite extent. Figure 9 demonstrates the variation of phase angle of the maximum magnetic intensity with dimensionless distance.

In the central portion of a finite system, the magnetic wave is similar to that produced by a system of infinite extent. Figure 8 shows that in most cases the effect of termination of a finite coil system is to raise or lower the axial magnetic flux density amplitude near the ends of the coil system toward that value of the amplitude produced by an isolated single-turn loop ($\bar{B}/B_0 = 1$). The difference between amplitudes at the center and at the ends of the system is increased with increasing values of coil-radius to magnetic-wave-wavelength ratio and with decreasing values of the number of phases or coils per wavelength. It is conceivable that these end effects could be reduced or eliminated through very careful variation of ampere turns with

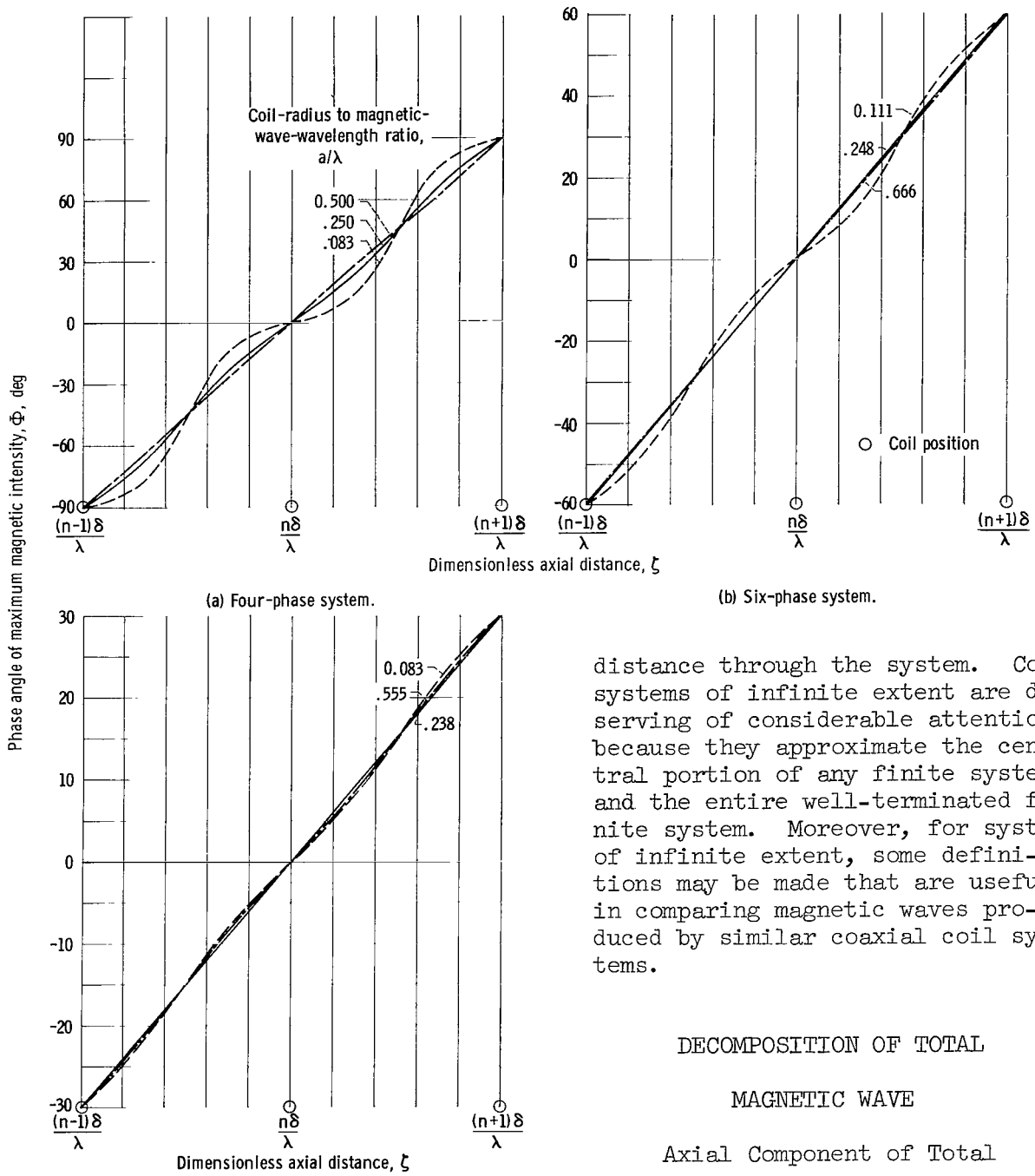

(a) Four-phase system.

(b) Six-phase system.

(c) Twelve-phase system.

Figure 7. - Phase-angle variation for coil systems of infinite extent.

distance through the system. Coil systems of infinite extent are deserving of considerable attention, because they approximate the central portion of any finite system and the entire well-terminated finite system. Moreover, for systems of infinite extent, some definitions may be made that are useful in comparing magnetic waves produced by similar coaxial coil systems.

DECOMPOSITION OF TOTAL MAGNETIC WAVE

Axial Component of Total Magnetic Wave

A more detailed understanding of traveling magnetic waves produced by coil systems of infinite extent was obtained by decomposing the total wave into a system of

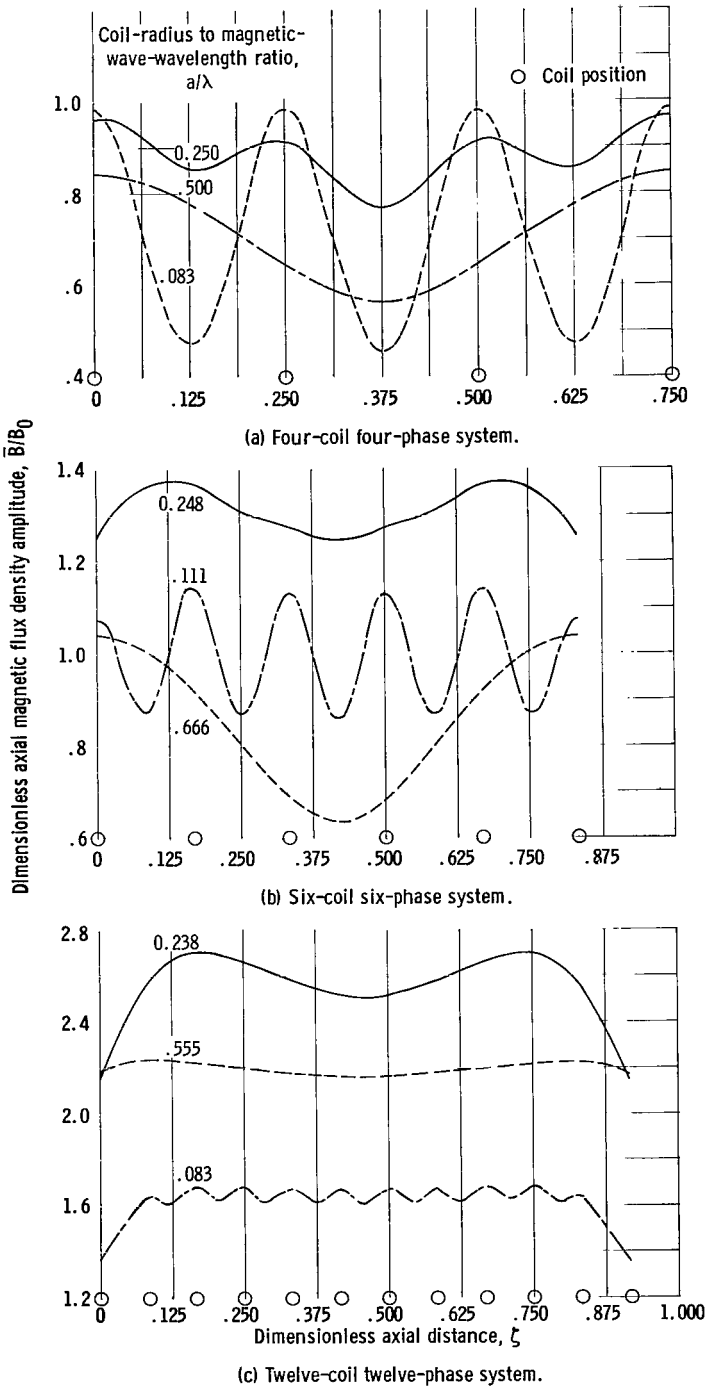

Figure 8. - Magnetic intensity envelopes for coil systems of finite extent.

constant-velocity constant-amplitude waves running in both directions. Such a system can be represented by the series

$$\frac{B_z}{B_0} = \sum_{1}^{\infty} f_m \cos(\omega t - 2\pi m\zeta) + \sum_{1}^{\infty} g_m \cos(\omega t + 2\pi m\zeta) \qquad (25)$$

where the coefficients f_m are the amplitudes of the forward, or downstream-running, magnetic waves and the coefficients g_m are the amplitudes of the rearward, or upstream-running, magnetic waves. The m^{th} forward-running wave has the constant velocity $\omega\lambda/2\pi m$, while the m^{th} rearward-running wave has the velocity $-\omega\lambda/2\pi m$. All waves of the system are produced at the constant radial frequency ω.

It is shown in appendix C that

$$f_m = 2N \int_0^{\infty} F \cos 2\pi m\xi \, d\xi \qquad (C13a)$$

if $(m - 1)/N$ is an integer or

$$f_m = 0 \qquad (C13b)$$

if $(m - 1)/N$ is not an integer, and

$$g_m = 2N \int_0^{\infty} F \cos 2\pi m\xi \, d\xi \qquad (C14a)$$

if $(m + 1)/N$ is an integer or

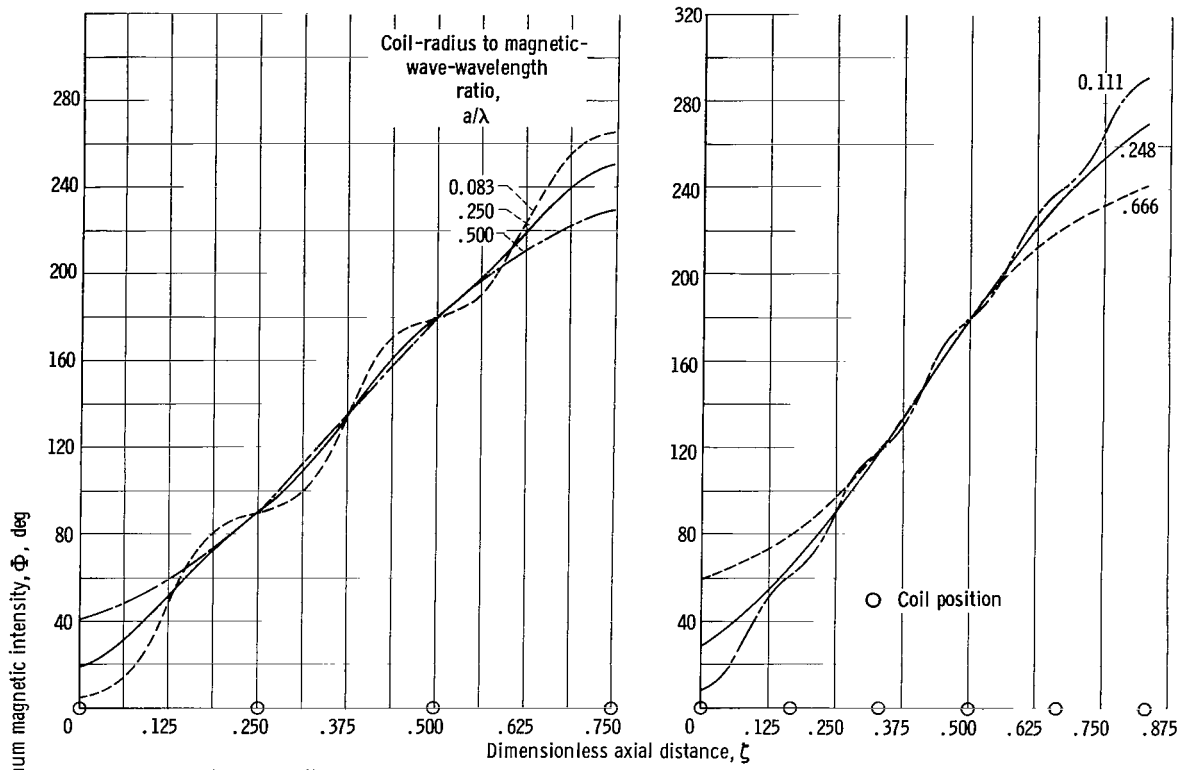

(a) Four-coil four-phase system.

(b) Six-coil six-phase system.

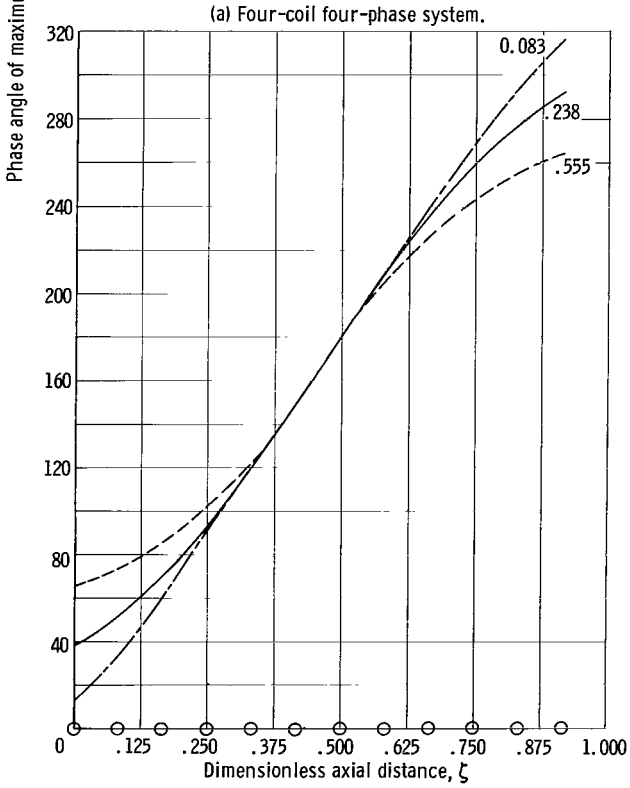

(c) Twelve-coil twelve-phase system.

Figure 9. - Phase-angle variation for coil systems of finite extent.

$$g_m = 0 \qquad \text{(C14b)}$$

if $(m + 1)/N$ is not an integer.

To eliminate terms from equations (C13) and (C14) that are identically zero, new sets of integers $\bar{m}$ are defined so that equation (25) becomes

$$\frac{B_z}{B_0} = \sum_{\bar{m}=0}^{\infty} \bar{f}_{\bar{m}} \cos\left[\omega t - 2\pi(\bar{m}N + 1)\zeta\right] + \sum_{\bar{m}=1}^{\infty} \bar{g}_{\bar{m}} \cos\left[\omega t + 2\pi(\bar{m}N - 1)\zeta\right] \qquad (26)$$

where

$$\bar{f}_{\bar{m}} = 2N \int_0^{\infty} F \cos 2\pi(\bar{m}N + 1)\xi \, d\xi \tag{27}$$

and

$$\bar{g}_{\bar{m}} = 2N \int_0^{\infty} F \cos 2\pi(\bar{m}N - 1)\xi \, d\xi \tag{28}$$

The coefficient $\bar{f}_0$ represents the amplitude of the design wave, which is a forward-running wave with the design velocity $\omega\lambda/2\pi$. For all the other values of $\bar{m}$, there exist both a downstream-running wave and an upstream-running wave that have velocities of $\omega\lambda/2\pi(N\bar{m} + 1)$ and $-\omega\lambda/2\pi(N\bar{m} - 1)$, respectively.

Equations (27) and (28) were programed for integration on a digital computer, and the values of $\bar{f}_{\bar{m}}$ and $\bar{g}_{\bar{m}}$ corresponding to the first three waves of the system are shown in table II for a wide variation in the coil-radius to

TABLE II. - RESULTS OF FOURIER ANALYSIS

Number of phases or coils per wavelength, N	Ratio of coil-radius to magnetic-wave-wavelength, a/λ	Fourier amplitude for -			Dimensionless axial magnetic flux density amplitude, $\bar{B}/B_0$	
		Design magnetic wave, $\bar{f}_0$	First detrimental forward-running wave, $\bar{f}_1$	First detrimental rearward-running wave, $\bar{g}_1$	Average	Maximum deviation from average
12	0.555	1.0464	0.0	0.0	1.0472	0.0
	.333	2.0716	.0	.0	2.0716	.0
	.238	2.3849	.0	.0	2.3850	.0
	.111	1.9628	.0012	.0045	1.9631	.0068
	.083	1.6346	.0076	.0201	1.6347	.0277
	.055	1.1948	.0410	.0768	1.1962	.1166
	.042	.9322	.0847	.1336	.9328	.2096
	.028	.6426	.1495	.1990	.6438	.3003
6	0.666	0.3373	0.0	0.0	0.3377	0.0
	.338	1.0358	.0	.0004	1.0358	.0005
	.248	1.1829	.0002	.0044	1.1818	.0045
	.222	1.2012	.0006	.0086	1.2012	.0092
	.167	1.1645	.0047	.0326	1.1646	.0374
	.111	.9814	.0299	.1046	.9828	.1332
	.083	.8173	.0673	.1672	.8204	.2243
	.055	.5974	.1292	.2289	.6018	.3112
4	0.500	0.4262	0.0	0.0013	0.4261	0.0012
	.333	.6906	.0003	.0165	.6906	.0169
	.250	.7878	.0028	.0526	.7885	.0548
	.166	.7763	.0217	.1420	.7810	.1650
	.125	.6960	.0533	.2084	.7048	.2699
	.083	.5448	.1114	.2626	.5561	.3311

magnetic-wave-wavelength ratio, and for four, six, and twelve coils per wavelength. For simplicity, these calculations were done at a value of the dimensionless radial coordinate equal to zero. These values are accurate to five

significant figures. It is noted in table II that the average values of the dimensionless axial magnetic flux density amplitude correspond closely to the tabulated values of the amplitude of the design wave. It is further noted that the values of the deviation of the dimensionless axial magnetic flux density amplitude about the average are approximately equal to the sum of the amplitudes of the first detrimental forward- and rearward-running waves, respectively, ($\overline{f}_1$ and $\overline{g}_1$).

It is apparent that equations (23) and (27) are equivalent when $\overline{m}$ is zero. Thus, for the limiting situation of an infinite number of phases per wavelength, the entire wave consists simply of the design wave. This is the natural result of the constant magnetic intensity envelope coupled with a linear variation of the phase angle with axial distance.

Radial Component of Magnetic Wave

Equations (26) to (28) completely describe the axial magnetic field for infinite coil systems; however, the actual plasma acceleration process is produced by the radial component of the magnetic field.

From Maxwell's divergence equation,

$$\frac{B_r}{B_0} = -\frac{1}{\rho}\frac{a}{\lambda}\int_0^{\rho} \rho \frac{\partial}{\partial \zeta}\left(\frac{B_z}{B_0}\right) \tag{29}$$

where B_r/B_0 is the dimensionless radial component of the magnetic field. Differentiating equation (26), substituting into equation (29), and performing the indicated integration give

$$\frac{B_r}{B_0} = -\pi\rho\frac{a}{\lambda}\left\{\sum_0^{\infty}(\overline{m}N + 1)\overline{f_m}\sin\left[\omega t - 2\pi(\overline{m}N + 1)\zeta\right] - \sum_1^{\infty}(\overline{m}N - 1)\overline{g_m}\sin\left[\omega t + 2\pi(\overline{m}N - 1)\zeta\right]\right\} \tag{30}$$

This expression will be used in the subsequent definitions and discussion of magnetic-wave quality factors.

QUALITY FACTOR DEFINITIONS

Total Quality Factor

It is desirable to define a figure of merit that will be useful in comparing magnetic waves produced by similar coaxial coil systems. This figure of merit, or total quality factor, represents, for a wavelength of the accelera-

tor, the net average energy in the radial component of the magnetic wave available for useful plasma acceleration for a given coil power consumption.

The total magnetic wave is composed of the design wave and an infinite number of slower upstream-running waves and downstream-running waves. Since it is desirable to accelerate the plasma to the design wave speed, all other waves tend to hamper the acceleration process. Thus, the net average energy available for useful plasma acceleration is taken to be the difference between the energy in the design wave and the energy in all other waves. It is, therefore, convenient to define the total quality factor Q as the product of two individual quality factors $Q = Q_L Q_R$. The first, the level quality factor Q_L accounts for the magnetic energy in the design wave for a given coil power consumption. The other, the ripple quality factor Q_R, accounts for the fraction of energy that is unavailable for useful plasma acceleration because of the presence of undesirable waves. On an approximate basis, the level quality factor accounts for the magnitude of the average magnetic intensity, while the ripple quality factor accounts for the deviations of the amplitude and the slope of the phase from their mean values. It is convenient to make all calculations of these factors for coil systems of infinite extent to avoid the complications of end effects.

Level Quality Factor

The level quality factor Q_L accounts for the variation in the magnetic intensity level of the design wave and is defined as the average magnetic energy contained in the radial field of the design wave for a given amount of average power consumed in the coil system per wavelength; that is,

$$Q_L = \frac{\frac{\omega}{2\pi}\int_0^{\frac{2\pi}{\omega}}\int_{V_1}\frac{B_{r,0}^2}{2\mu}\,dV_1\,dt}{\frac{\omega}{2\pi}\int_0^{\frac{2\pi}{\omega}}\int_{V_2} J^2 R\,dV_2\,dt} \tag{31}$$

where $B_{r,0}$ is the radial component of the design wave, J is the current density, and R is the resistivity of the coil material. The volume V_1 refers to the cylindrical volume of a one-wavelength section of plasma accelerator, while volume V_2 refers to a one-wavelength section of the coil system.

The numerator of equation (31) may be evaluated by utilizing equation (30) to determine the radial component of the design magnetic wave. Thus,

$$B_{r,0}^2 = \left(\pi\rho \frac{a}{\lambda} \bar{f}_0 B_0\right)^2 \sin^2(\omega t - 2\pi\zeta) \tag{32}$$

where $\bar{m} = 0$.

The incremental annular volume dV_1 in nondimensional cylindrical coordinates is

$$dV_1 = 2\pi a^2 \lambda \rho \, d\rho \, d\zeta \tag{33}$$

The limits on the nondimensional variables in the integration shown in the numerator of equation (31) are from $\zeta = \zeta_0$ to $\zeta_0 + 1$, one wavelength of the accelerator; and from $\rho = 0$ to ρ_0, the dimensionless radius of the plasma accelerator. Substitution of equations (32) and (33) into (31) yields, for the numerator,

$$\frac{\omega}{2\pi} \int_0^{2\pi} \int_{V_1} \frac{B_{r,0}^2}{2\mu} \, dV_1 \, dt = \frac{\rho_0^2 I_1^2}{2} \frac{\pi^3 a^4 B_0^2 N^2}{\mu\lambda} \left[1 - \frac{4I_2}{I_1} \rho_0^2 + O(\rho_0^4)\right] \tag{34}$$

where

$$I_1 = \int_0^\infty b^{-3/2} \cos 2\pi\xi \, d\xi$$

and

$$I_2 = \int_0^\infty \left(b^{-5/2} - \frac{5}{4} b^{-7/2} \cos\right) 2\pi\xi \, d\xi$$

The denominator of equation (31) is merely the average ohmic heating loss in a one-wavelength section of the coil system. It is the product of the square of the root-mean-square current, the resistance of an individual coil, and the number of coils per wavelength; that is,

$$\frac{\omega}{2\pi} \int_0^{\frac{2\pi}{\omega}} \int_{V_2} J^2 R \, dV_2 \, dt = \frac{\pi a I_0^2 R N}{A_c} \tag{35}$$

where A_c is the current-carrying cross-sectional area of a coil.

The substitution of equations (34) and (35) and the defining relation for the magnetic flux density B_0 into equation (31) yields, for the level quality factor,

$$Q_L = \frac{\pi^2 \mu \rho_0^4 I_1^2}{8} \frac{a}{\lambda} \frac{A_c N}{R} \left[1 - \frac{4I_2}{I} \rho_0^2 + O(\rho_0^4) \right] \tag{36}$$

Thus, for systems with the same ratio of accelerator to coil radius ρ_0 and the same ratio of total-current-carrying cross-sectional area per wavelength to resistivity $A_c N/R$, the result is

$$Q_L \propto \frac{a}{\lambda} I_1^2 \left[1 - 4\rho_0^2 \frac{I_2}{I_1} + O(\rho_0^4) \right] \tag{37}$$

Ripple Quality Factor

The ripple quality factor Q_R accounts for the presence of magnetic waves other than the design wave. This factor is the fraction of the average power contained in the radial component of the design magnetic wave that is actually useful for efficient acceleration of the plasma:

$$Q_R = 1 - \frac{\int_0^{\frac{2\pi}{\omega}} \int_{V_1} \left(B_r^2 - B_{r,0}^2 \right) dV_1 \, dt}{\int_0^{\frac{2\pi}{\omega}} \int_{V_1} B_{r,0}^2 \, dV_1 \, dt} \tag{38}$$

The presence of waves other than the design wave is considered detrimental to the best operation of the plasma accelerator. Upstream-running waves are obviously detrimental because they run counter to the plasma flow. Downstream-running waves, other than the design wave, are considered undesirable because they are slower than the design wave and thus tend to limit the plasma velocity to speeds slower than the design wave speed.

For the cases where the undesirable waves are not large compared with the design wave, the total magnetic wave is adequately represented by the first three terms in equation (30). These terms are for $\bar{m} = 0$ (the design wave) and for $\bar{m} = 1$ (the dominant upstream- and downstream-running waves). Thus, substituting the first three terms of equation (30) into equation (38) and integrating, using the defining relations of equations (33), (27), (28), and (C8), give

$$Q_R = 1 - \left\{ (N+1)^2 \left(\frac{I_1'}{I_1} \right)^2 \left[\left(1 - 4\rho_0^2 \frac{I_2'}{I_1'} \right) \Big/ \left(1 - 4\rho_0^2 \frac{I_2}{I_1} \right) \right] + (N-1)^2 \left(\frac{I_1''}{I_1} \right)^2 \left[\left(1 - 4\rho_0^2 \frac{I_2''}{I_1''} \right) \Big/ \left(1 - 4\rho_0^2 \frac{I_2}{I_1} \right) \right] \right\} \tag{39}$$

where

$$I_1' = \int_0^\infty b^{-3/2} \cos 2\pi(N + 1)\xi \, d\xi$$

$$I_1'' = \int_0^\infty b^{-3/2} \cos 2\pi(N - 1)\xi \, d\xi$$

$$I_2' = \int_0^\infty \left[b^{-5/2} - \frac{5}{4} b^{-7/2}\right] \cos 2\pi(N + 1)\xi \, d\xi$$

and

$$I_2'' = \int_0^\infty \left[b^{-5/2} - \frac{5}{4} b^{-7/2}\right] \cos 2\pi(N - 1)\xi \, d\xi$$

RESULTS AND DISCUSSION OF QUALITY FACTORS

Level Quality Factor

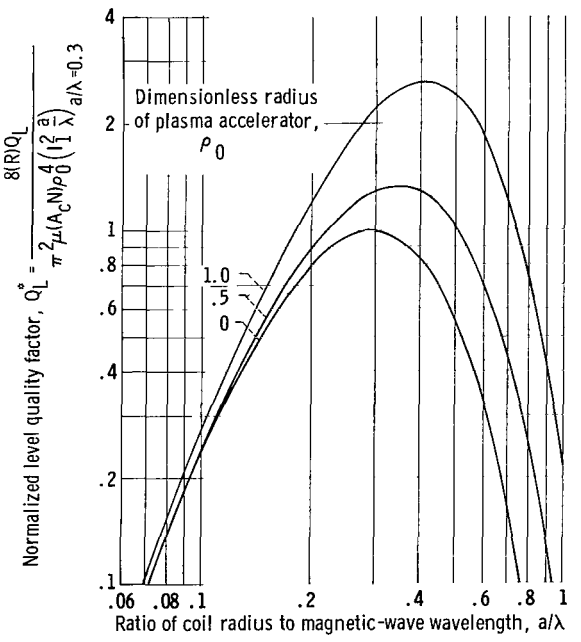

Figure 10. - Normalized level quality factor as function of ratio of coil radius to magnetic-wave wavelength.

Equation (36) demonstrates the dependence of the level quality factor Q_L on the system parameters. For particular values of the dimensionless radius of the plasma accelerator ρ_0, expression (37), which is completely independent of the number of phases or coils per wavelength, may be used to obtain a graphical representation of level quality factor against coil radius to wavelength ratio for all similar coil systems, that is, for coil systems for which the ratio of the total-current-carrying cross-sectional area per wavelength to resistivity A_cN/R and the dimensionless radius of the plasma accelerator ρ_0 are the same. Similar coil systems are compared on the basis that the conductor materials are the same and that the mass of conductor material per wavelength (proportional to A_cN) is the

same. The growth of expression (37) with increasing plasma accelerator radius is shown in figure 10. The values of

$$\frac{a}{\lambda} I_1^2 \left(1 - 4\rho_0^2 \frac{I_2}{I_1}\right)$$

shown in figure 10 are relative, having been normalized with respect to the value obtained at a coil-radius to magnetic-wave-wavelength ratio equal to 0.3 and a plasma accelerator radius equal to zero for convenience of display. Since the approximation used to obtain the radial flux density is accurate to values of plasma accelerator radius equal to 0.5, the values from expression (37) are also accurate only to this value. The case where the plasma accelerator radius is equal to 1 is shown here, as well as in subsequent calculations, to indicate the trend of the peak values of expression (37).

Figure 10 shows that expression (37) optimizes at some value of the ratio of coil radius to magnetic-wave wavelength. This optimum tends to shift toward larger values of the coil radius to wavelength ratio as the plasma accelerator radius is increased. For all systems with a plasma accelerator radius equal to or less than 0.5, the optimum value of the coil radius to wavelength ratio lies between 0.30 and 0.35.

Thus, for all similar coaxial coil systems, an optimum magnetic wavelength is determined that maximizes the design magnetic wave and is completely independent of the number of phases per wavelength.

Equation (36), the general expression for the level quality factor, may be considered a scaling law for all coil systems. Therefore, more efficient use of electrical energy may be gained by letting the plasma accelerator radius ratio approach 1, the total-current-carrying cross-sectional area per wavelength increase, and the resistivity of the coil decrease; that is, coils should be located as close to the accelerator wall as possible, the current-carrying cross-sectional area per wavelength should be as large as possible, and, of course, the coil conductor resistivity should be as small as possible. Furthermore, equation (36) shows that a general increase in the size of the system yields an increase in the level quality factor. That is, with an increase in the coil radius and with the plasma accelerator radius and coil radius to wavelength ratio held constant, it becomes geometrically possible to increase the current-carrying cross-sectional area of the coil appreciably. The level quality factor can, therefore, be increased with increasing accelerator size even for those systems where conductor resistance is determined by high-frequency skin effects, since an increase in conductor surface area tends to decrease the conductor resistance.

Ripple Quality Factor

For all the cases considered in this report, the total magnetic wave is adequately represented by the sum of the first three waves. Thus, equation (39) is valid for the computation of the ripple quality factor. Figure 11 shows plots of ripple quality factor against coil radius to wavelength ratio

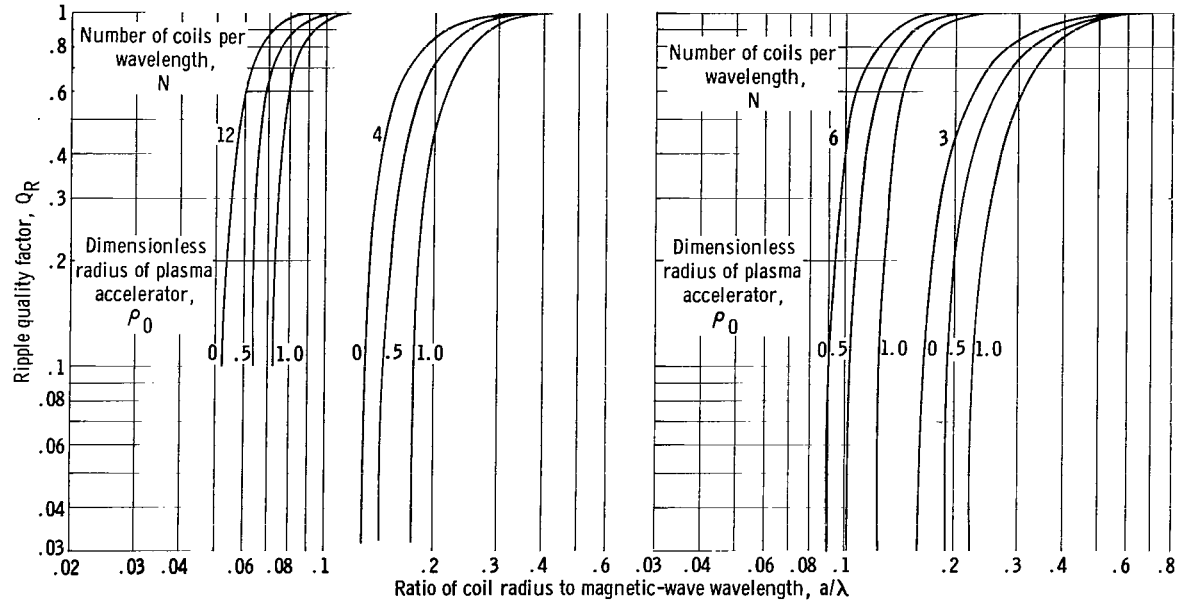

(a) Four- and twelve-coil systems. (b) Three- and six-coil systems.

Figure 11. - Ripple quality factor as function of ratio of coil radius to magnetic-wave wavelength.

for variously phased systems for values of the plasma accelerator radius of 0, 0.5, and 1.0. In the limiting case of an infinite number of phases per wavelength, the ripple quality factor is 1.0 for all values of coil radius to wavelength ratio and plasma accelerator radius. In general, however, the ripple quality factor rises sharply, approaching a value of 1.0 at some value of the coil radius to wavelength ratio that decreases as the number of coils per wavelength increases and the plasma accelerator radius decreases. Thus, the effect of increasing the number of phases per wavelength is to diminish the undesirable waves.

Total Quality Factor

The product of equations (37) and (39) is proportional to Q, the total quality factor, which is plotted against the coil radius to wavelength ratio in figure 12 for variously phased similar coil systems with values of the plasma accelerator radius of 0, 0.5, and 1.0. It is seen that a family of curves with a common maximum point at a value of the coil radius to wavelength ratio between 0.3 and 0.4 is generated at each value of the plasma accelerator radius when the number of phases per wavelength is greater than three. As the ratio of coil radius to the wavelength increases, each curve asymptotically approaches the curve for the number of phases per wavelength equal to infinity. In the vicinity of the optimum value of the coil radius to wavelength ratio, the number of phases per wavelength plays an insignificant role in the total quality factor when that number is greater than three. Therefore, the most efficient production of useful magnetic energy is assured primarily by the proper selection of the coil radius to wavelength ratio, but the use of a plasma accelerator with a very large number of phases does not of itself guarantee efficient production of magnetic energy for plasma acceleration. Indeed,

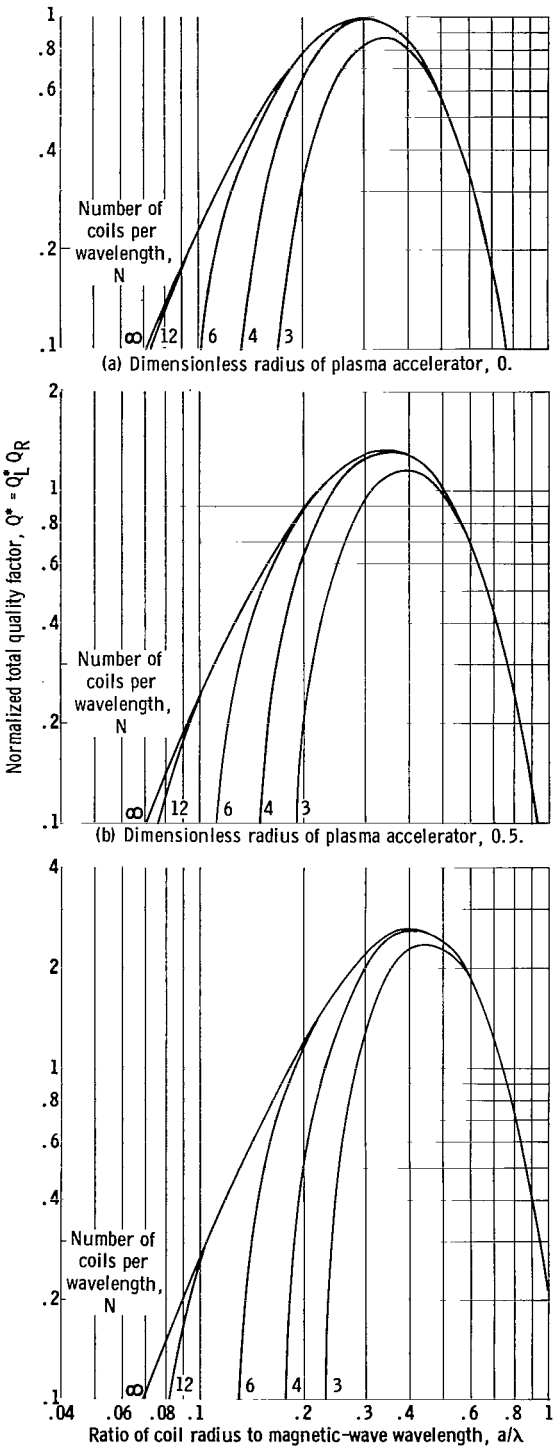

Figure 12. - Normalized total quality factor as function of ratio of coil radius to magnetic-wave wavelength.

such a large number of phases introduces unnecessary complexity in electrical design.

CONCLUSIONS

Analysis of the effect of several parameters on the design of a simple coaxial traveling magnetic-wave coil system showed that the efficiency of production of useful magnetic waves for plasma acceleration is independent of the number of phases per wavelength when that number is greater than three and is primarily dependent on the value of the ratio of the coil radius to the magnetic-wave wavelength. The optimum value of the ratio of the coil radius to the magnetic-wave wavelength was between 0.3 and 0.4. An approximate scaling law indicates that the efficiency of production of traveling magnetic waves should increase with increasing size of the coil system.

Lewis Research Center
National Aeronautics and Space Administration
Cleveland, Ohio, January 23, 1964

APPENDIX A

SYMBOLS

The mks system of units is used throughout this report.

A_c cross-sectional area of coil that carries current

$\mathscr{A}_m, \mathscr{B}_m$ Fourier coefficients

a radius of current carrying turn

B_0 magnetic flux density at geometric center of single-turn loop of radius a with current I_0; $B_0 = \mu I_0/2a$

B_r radial magnetic flux density

$B_{r,0}$ radial magnetic flux density of design magnetic wave

B_z axial magnetic flux density

$\overline{B}/B_0$ axial magnetic flux density amplitude, dimensionless

b $1 + (\lambda/a\overline{\xi})^2$

b_n $1 + \overline{d}_n^2$

$\overline{b}$ $1 + \overline{d}^2$

C_1 $\sum_{-n_-}^{n_+} F_n \sin \frac{2\pi n}{N}$

C_2 $\sum_{-n_-}^{n_+} F_n \cos \frac{2\pi n}{N}$

d axial distance from plane of coil to field point

$\overline{d}$ axial distance from plane of coil to field point, d/a, dimensionless

$\overline{d}_n$ axial distance from plane of n^{th} coil to field point, $\left|\frac{z - n\delta}{a}\right|$, dimensionless

E(k) complete elliptic integral of second kind

F $b^{-3/2}\left[1 - \rho^2\left(3b^{-1} - \frac{15}{4}\, b^{-2}\right)\right]$

F_n $b_n^{-3/2}\left[1 - \rho^2\left(3b_n^{-1} - \frac{15}{4}\, b_n^{-2}\right)\right]$

f_m set of Fourier amplitudes for forward-running waves

$\overline{f_m}$ nonzero Fourier amplitudes for forward-running waves

$\overline{f}_0$ Fourier amplitude for design magnetic wave

$\overline{f}_1$ Fourier amplitude for first detrimental forward-running wave

g_m set of Fourier amplitudes for rearward-running waves

$\overline{g_m}$ nonzero Fourier amplitudes for rearward-running waves

$\overline{g}_1$ Fourier amplitude for first rearward-running wave

I current

I_n current in n^{th} coil

I_0 maximum current in coil

J volume current density

j integer

$K(k)$ complete elliptic integral of first kind

k modulus for complete elliptic integrals; $k^2 = \frac{4ar}{(r + a)^2 + d^2}$, $k^2 < 1$

l integer

m summation index for Fourier analysis

$\overline{m}$ integer

N number of phases or coils per wavelength

n number of individual coil

n_T total number of coils, $n_+ + n_-$

$\overline{n}$ integer, $1 \leq \overline{n} \leq N$

Q_T total quality factor

Q_L level quality factor

Q_R	ripple quality factor
Q^*	normalized total quality factor
Q_L^*	normalized level quality factor
R	resistivity of coil material
R_0	radius of accelerator
r	radial coordinate
S	$\sum_{\overline{n}=1}^{N} \left[e^{2\pi i(\overline{m}/N)}\right]^{\overline{n}}$ (appendix D)
t	time
V_1	cylindrical volume of one-wavelength section of plasma accelerator
V_2	annular volume of one-wavelength section of coil system
z	axial coordinate
δ	distance between adjacent coils
ζ	axial coordinate, z/λ, dimensionless
λ	magnetic-wave wavelength
μ	magnetic permeability
$\xi, \overline{\xi}, \overline{\xi}_n$	dimensionless variables
ρ	radius ratio radial coordinate, r/a, dimensionless
ρ_0	plasma accelerator radius ratio, R_0/a, dimensionless
Φ	phase angle of maximum magnetic intensity
$\Delta\varphi$	constant electrical phase angle between adjacent coils
ω	angular frequency

APPENDIX B

APPROXIMATE MAGNETIC FIELD OF SINGLE-TURN LOOP

Equation (3) of the text may be rewritten as

$$\frac{B_z}{B_0} = \frac{I}{I_0 \pi} f(\rho,\bar{b}) \tag{B1}$$

where

$$f(\rho,b) = [\rho(\rho + 2) + \bar{b}]^{-1/2}\left[K + \frac{2 - \rho^2 - \bar{b}}{\rho(\rho - 2) + \bar{b}} E\right] \tag{B2}$$

The complete elliptic integrals of the first and second kind that appear in equation (B2) are given by the following series in k^2:

$$K = \frac{\pi}{2}\left[1 + \left(\frac{1}{2}\right)^2 k^2 + \left(\frac{1 \times 3}{2 \times 4}\right)^2 k^4 + \left(\frac{1 \times 3 \times 5}{2 \times 4 \times 6}\right)^2 k^6 + \cdots\right] \tag{B3}$$

and

$$E = \frac{\pi}{2}\left[1 - \left(\frac{1}{2}\right)^2 k^2 - \left(\frac{1 \times 3}{2 \times 4}\right)^2 \frac{k^4}{3} - \left(\frac{1 \times 3 \times 5}{2 \times 4 \times 6}\right)^2 \frac{k^6}{5} - \cdots\right] \tag{B4}$$

where k^2 is given by equation (6).

Equation (B2) can now be approximated by employing Maclaurin's series:

$$f(\rho,b) = f(0,\bar{b}) + \rho \frac{\partial f}{\partial \rho}(0,\bar{b}) + \frac{\rho^2}{2} \frac{\partial^2 f}{\partial \rho^2}(0,\bar{b}) + \cdots \tag{B5}$$

In equations (B6a) to (B6d) partial derivatives of K and E with respect to ρ must be taken implicitly and evaluated at $\rho = 0$. The first two derivatives are

$$\frac{\partial K}{\partial \rho}(0,\bar{b}) = \frac{\pi}{2\bar{b}} \tag{B6a}$$

$$\frac{\partial^2 K}{\partial \rho^2}(0,\bar{b}) = \frac{\pi}{4\bar{b}^2} \tag{B6b}$$

$$\frac{\partial E}{\partial \rho}(0,\bar{b}) = -\frac{\pi}{2\bar{b}} \tag{B6c}$$

$$\frac{\partial^2 E}{\partial \rho^2}(0,\bar{b}) = \frac{5\pi}{4\bar{b}^2} \tag{B6d}$$

Determining the indicated derivatives of equation (B5) by using the relations of (B6) gives

$$f(0,\bar{b}) = \frac{\pi}{\bar{b}^{3/2}} \tag{B7a}$$

$$\frac{\partial f}{\partial \rho}(0,\bar{b}) = 0 \tag{B7b}$$

$$\frac{\partial^2 f}{\partial \rho^2}(0,\bar{b}) = -\frac{\pi}{\bar{b}^{3/2}}\left(6\bar{b}^{-1} - \frac{15}{2}\bar{b}^{-2}\right) \tag{B7c}$$

Substituting relations (B7) into equations (B2) and (B1) and neglecting terms of order higher than ρ^2 yield, for the approximate axial field of a single-turn loop,

$$\frac{B_z}{B_0} = \frac{Ib^{-3/2}}{I_0}\left[1 - \rho^2\left(3\bar{b}^{-1} - \frac{15}{4}\bar{b}^{-2}\right)\right] \tag{B8}$$

A similar method could be used to compute an approximate expression for B_r/B_0, the dimensionless radial component of the magnetic field; however, since there is no azimuthal component of the total magnetic field from a single-turn loop, Maxwell's divergence equation and equation (B8) can be used to approximate the radial flux density with more ease.

The divergence equation in dimensional cylindrical coordinates for a single-turn loop is

$$\frac{1}{r}\frac{\partial}{\partial r}(rB_r) + \frac{\partial B_z}{\partial d} = 0 \tag{B9}$$

Thus, in terms of the dimensionless variables $\bar{d}$ and ρ,

$$\frac{B_z}{B_0} = -\frac{1}{\rho}\int_0^{\rho} \rho \frac{\partial}{\partial \bar{d}}\left(\frac{B_z}{B_0}\right)d\rho \tag{B10}$$

Partial differentiation of equation (B8) with respect to $\bar{d}$ and substitution into equation (B10) result in

$$\frac{B_r}{B_0} = \frac{3}{2}\rho\left(\frac{\bar{b}-1}{\bar{b}^5}\right)^{1/2}\frac{I}{I_0}\left[1 - \frac{5}{2}\rho^2\bar{b}^{-1}\left(1 - \frac{7}{4}\bar{b}^{-1}\right)\right] \tag{B11}$$

APPENDIX C

FOURIER EXPANSION OF TOTAL MAGNETIC WAVE

For coil systems of infinite extent, it becomes convenient to substitute

$$n = Nj + \bar{n} \qquad \begin{cases} -\infty \le j \le +\infty \\ 1 \le \bar{n} \le N \end{cases} \tag{C1}$$

into equation (15) and perform the double sum, first over the number of coils in a magnetic wavelength, and then over the number of wavelengths in the total system:

$$\frac{B_z}{B_0} = \sum_{j=-\infty}^{\infty} \sum_{\bar{n}=1}^{N} F_n \cos\left[\omega t - 2\pi\left(j + \frac{\bar{n}}{N}\right)\right] \tag{C2}$$

where

$$F_n = b_n^{-3/2}\left[1 - \rho^2\left(3b_n^{-1} - \frac{15}{4} b_n^{-2}\right)\right]$$

and

$$b_n = 1 + \left(\frac{\lambda}{a}\right)^2\left(\zeta - j - \frac{\bar{n}}{N}\right)^2$$

The assumed form of the Fourier expansion given by equation (25) is

$$\frac{B_z}{B_0} = \sum_{m=1}^{\infty} f_m \cos(\omega t - 2\pi m\zeta) + \sum_{m=1}^{\infty} g_m \cos(\omega t + 2\pi m\zeta) \tag{C3}$$

Equating (C2) and (C3), expanding the trigonometric functions, and noting that the coefficients of $\cos \omega t$ and $\sin \omega t$ terms must be zero result in

$$\sum_{j=-\infty}^{\infty} \sum_{\bar{n}=1}^{N} F_n \begin{Bmatrix} \cos \\ \sin \end{Bmatrix} 2\pi \frac{\bar{n}}{N} = \sum_{1}^{\infty} \begin{Bmatrix} \mathscr{B}_m \cos \\ \mathscr{A}_m \sin \end{Bmatrix} 2\pi m\zeta \tag{C4}$$

where

$$\begin{Bmatrix} \mathscr{A}_m \\ \mathscr{B}_m \end{Bmatrix} = f_m \mp g_m \tag{C5}$$

If equation (C4) is multiplied by $\begin{Bmatrix} \cos \\ \sin \end{Bmatrix} 2\pi l\zeta$, where l is an integer, and is

integrated from $\zeta = 0$ to 1, the result is

$$\begin{Bmatrix} \mathscr{A}_m \\ \mathscr{B}_m \end{Bmatrix} = 2 \int_{\zeta=0}^{1} \sum_{j=-\infty}^{\infty} \sum_{\overline{n}=1}^{N} F_n \begin{Bmatrix} \sin \\ \cos \end{Bmatrix} 2\pi \frac{\overline{n}}{N} \begin{Bmatrix} \sin \\ \cos \end{Bmatrix} 2\pi m\zeta \, d\zeta \tag{C6}$$

Define

$$\xi = \zeta - j - \frac{\overline{n}}{N} \tag{C7}$$

Substituting equation (C7) into (C6) and exchanging summation and integration yield

$$\begin{Bmatrix} \mathscr{A}_m \\ \mathscr{B}_m \end{Bmatrix} = 2 \sum_{\overline{n}=1}^{N} \sum_{j=-\infty}^{\infty} \int_{-j-\overline{n}/N}^{1-j-\overline{n}/N} F \begin{Bmatrix} \sin \\ \cos \end{Bmatrix} 2\pi \frac{\overline{n}}{N} \begin{Bmatrix} \sin \\ \cos \end{Bmatrix} 2\pi m \left(\xi + \frac{\overline{n}}{N} \right) d\xi \tag{C8}$$

where

$$F = b^{-3/2} \left[1 - \rho^2 \left(3b^{-1} - \frac{15}{4} b^{-2} \right) \right]$$

and

$$b = 1 + \left(\frac{\lambda}{a} \right)^2 \xi^2$$

When it is noted that

$$\sum_{j=-\infty}^{\infty} \int_{-j-\overline{n}/N}^{1-j-\overline{n}/N} \mathscr{F}\left(\xi, \overline{n}, \rho, \frac{a}{\lambda} \right) d\xi = \int_{-\infty}^{\infty} \mathscr{F}\left(\xi, \overline{n}, \rho, \frac{a}{\lambda} \right) d\xi \tag{C9}$$

the following trigonometric identity is used

$$\begin{Bmatrix} \sin \\ \cos \end{Bmatrix} 2\pi \frac{\overline{n}}{N} \begin{Bmatrix} \sin \\ \cos \end{Bmatrix} 2\pi m \left(\xi + \frac{\overline{n}}{N} \right) = \frac{1}{2} \cos 2\pi m\xi \left[\cos 2\pi \frac{\overline{n}}{N} (1 - m) \mp \cos 2\pi \frac{\overline{n}}{N} (1 + m) \right]$$

$$\pm \frac{1}{2} \sin 2\pi m\xi \left[\sin 2\pi \frac{\overline{n}}{N} (1 + m) + \sin 2\pi \frac{\overline{n}}{N} (1 - m) \right] \tag{C10}$$

and the symmetry of the resultant integrals is used, equation (C8) becomes

$$\begin{Bmatrix} \mathscr{A}_m \\ \mathscr{B}_m \end{Bmatrix} = 2 \left\{ \sum_{\bar{n}=1}^{N} \left[\cos 2\pi \frac{\bar{n}}{N}(1 - m) \mp \cos 2\pi \frac{\bar{n}}{N}(1 + m) \right] \right\} \int_0^\infty F \cos 2\pi m\xi \, d\xi \tag{C11}$$

Solving equation (C5) for f_m and g_m and substituting (C11) yield

$$\begin{Bmatrix} f_m \\ g_m \end{Bmatrix} = 2 \left[\sum_{\bar{n}=1}^{N} \cos 2\pi \frac{\bar{n}}{N}(1 \mp m) \right] \int_0^\infty F \cos 2\pi m\xi \, d\xi \tag{C12}$$

From appendix D,

$$\sum_{\bar{n}=1}^{\infty} \cos 2\pi \frac{\bar{n}}{N} \bar{m} = N$$

if $\bar{m}/N$ is an integer or

$$\sum_{\bar{n}=1}^{\infty} \cos 2\pi \frac{\bar{n}}{N} \bar{m} = 0$$

if $\bar{m}/N$ is not an integer. Thus,

$$f_m = 2N \int_0^\infty F \cos 2\pi m\xi \, d\xi \tag{C13a}$$

if $(m - 1)/N$ is an integer or

$$f_m = 0 \tag{C13b}$$

if $(m - 1)/N$ is not an integer, and

$$g_m = 2N \int_0^\infty F \cos 2\pi m\xi \, d\xi \tag{C14a}$$

if $(m + 1)/N$ is an integer or

$$g_m = 0 \qquad \text{(C14b)}$$

if $(m + 1)/N$ is not an integer.

APPENDIX D

PROPERTIES OF $\sum_{\bar{n}=1}^{N} \cos \frac{2\pi\bar{n}}{N} \bar{m}$

To evaluate $\sum_{\bar{n}=1}^{N} \cos \frac{2\pi\bar{n}}{N} \bar{m}$, where $\bar{m}$ is an arbitrary integer, let

$$\sum_{\bar{n}=1}^{N} \cos \frac{2\pi\bar{n}}{N} \bar{m} = \text{real part of } S \tag{D1}$$

where

$$S = \sum_{\bar{n}=1}^{N} \left[e^{2\pi i(\bar{m}/N)}\right]^{\bar{n}} \tag{D2}$$

Note that S is the sum of a finite geometric progression. Substitution of the terms of equation (D2) into the standard formula for obtaining the value of S yields

$$S = \frac{e^{2\pi i\bar{m}/N}\left(1 - e^{2\pi i\bar{m}}\right)}{1 - e^{2\pi i(\bar{m}/N)}} \tag{D3}$$

Thus,

$$S\left(1 - e^{2\pi i\bar{m}/N}\right) = e^{2\pi i\bar{m}/N}\left(1 - e^{2\pi i\bar{m}}\right) = 0 \tag{D4}$$

since $\bar{m}$ is an integer and $e^{2\pi i\bar{m}} = 1$. Thus, $S = 0$ if $e^{2\pi i\bar{m}/N} \neq 1$. But $e^{2\pi i\bar{m}/N} = 1$ if and only if $\bar{m}/N$ is an integer. Therefore, $S = 0$ if $\bar{m}/N$ is not an integer, and from equation (D1)

$$\sum_{\bar{m}=1}^{N} \cos \frac{2\pi\bar{m}}{N} \bar{m} = 0 \tag{D5}$$

if $\overline{m}/N$ is not an integer; however, if $\overline{m}/N$ is an integer

$$\cos 2\pi \frac{\overline{m}}{N} \overline{n} = 1 \tag{D6}$$

and

$$\sum_{n=1}^{N} \cos \frac{2\pi \overline{n}}{N} \overline{m} = N \tag{D7}$$

REFERENCES

1. Jones, Robert E., and Palmer, Raymond W.: Traveling Wave Plasma Engine Program at NASA Lewis Research Center. Paper presented at Third Annual Conf. on Eng. Aspects of Magnetohydrodynamics, Univ. Rochester, Mar. 28-29, 1962.

2. Covert, Eugene E., and Haldeman, Charles W.: The Traveling-Wave Pump. ARS Jour., vol. 31, no. 9, Sept. 1961, pp. 1252-1259.

3. Janes, G. Sargent: Magnetohydrodynamic Propulsion. Res. Rep. 90, Avco-Everett Res. Lab., Aug. 1960.

4. Weber, Ernst: Electromagnetic Fields; Theory, and Applications. John Wiley & Sons, Inc., 1950, p. 141.

e 7185

"The National Aeronautics and Space Administration . . . shall . . . provide for the widest practical appropriate dissemination of information concerning its activities and the results thereof . . . objectives being the expansion of human knowledge of phenomena in the atmosphere and space."

—NATIONAL AERONAUTICS AND SPACE ACT OF 1958

NASA SCIENTIFIC AND TECHNICAL PUBLICATIONS

TECHNICAL REPORTS: Scientific and technical information considered important, complete, and a lasting contribution to existing knowledge.

TECHNICAL NOTES: Information less broad in scope but nevertheless of importance as a contribution to existing knowledge.

TECHNICAL MEMORANDUMS: Information receiving limited distribution because of preliminary data, security classification, or other reasons.

CONTRACTOR REPORTS: Technical information generated in connection with a NASA contract or grant and released under NASA auspices.

TECHNICAL TRANSLATIONS: Information published in a foreign language considered to merit NASA distribution in English.

TECHNICAL REPRINTS: Information derived from NASA activities and initially published in the form of journal articles or meeting papers.

SPECIAL PUBLICATIONS: Information derived from or of value to NASA activities but not necessarily reporting the results of individual NASA-programmed scientific efforts. Publications include conference proceedings, monographs, data compilations, handbooks, sourcebooks, and special bibliographies.

Details on the availability of these publications may be obtained from:

SCIENTIFIC AND TECHNICAL INFORMATION DIVISION

NATIONAL AERONAUTICS AND SPACE ADMINISTRATION

Washington, D.C. 20546